

# Propane oxidative dehydrogenation over metal pyrophosphates catalysts

B.Y. Jibril, S.M. Al-Zahrani\* and A.E. Abasaheed

Chemical Engineering Department, King Saud University, PO Box 800, Riyadh 11421, Saudi Arabia

E-mail: szahrani@ksu.edu.sa

Received 1 February 2001; accepted 26 April 2001

Metal pyrophosphates ( $M-P_2O_7$ , where M is V, Zr, Cr, Mg, Mn, Ni or Ce) have been found to catalyze the oxidative dehydrogenation of propane to propene. The reaction was conducted at 1 atm, 450–550 °C and feed flowrate of 75 cm<sup>3</sup>/min (20 cm<sup>3</sup>/min propane, 5 cm<sup>3</sup>/min oxygen and the balance is helium). All catalysts showed increase in degrees of conversion and decrease in olefins selectivity with increase in reaction temperature. At 550 °C,  $MnP_2O_7$  exhibited the highest activity (40.7% conversion) and total olefins ( $C_3H_6$  and  $C_2H_4$ ) yield (29.3%). The other catalysts, indicated by their respective metals, may be ranked (based on olefins yield) as V (16.9%) < Cr (17.5%) < Ce (25.1%) < Zr (26.2%) < Ni (26.8%) < Mg (27.9%). The reactivity of the lattice oxygen was estimated from energy of formation of the corresponding metal oxides. Correlation between the selectivity to propene and the standard energy of formation was attempted. Although there was no clear correlation, the result suggested that the lattice oxygen play a key role in the selectivity-determining step.

**KEY WORDS:** metal pyrophosphates; reactivity of lattice oxygen; oxidative dehydrogenation of propane; propene from propane

## 1. Introduction

In a continuous effort to meet the future demands of chemicals, fibers and polymers, research interest has been shifted from using alkenes as feedstock to the cheap and more abundant alkanes. One approach is the oxidative dehydrogenation of alkanes to alkenes, which may then be further reacted for the production of more useful products. The catalytic oxidative dehydrogenation of propane (POD) has received extensive research efforts. This led to the discovery of several promising catalysts. The most studied catalytic systems for the reaction are based on vanadium [1,2], vanadium antimony [3], metal tungstates [4], metal molybdates [5,6] and phosphates [7,8]. Recently, rare earth vanadates have been reported to have better performance than the much-studied V–Mg–O systems [9].

In previous studies [10,11] we have investigated the activities of  $\gamma-Al_2O_3$ -supported transition metals (Cr, Mn, Zr, Ni and Y); Ba and rare earth metals (Dy, Tb, Yb, Ce, Tm, Ho and Pr) oxides for POD. They were found to catalyze the reaction at 350–450 °C, 1 atm and feed rate of 75 cm<sup>3</sup>/min of a mixture of  $C_3H_8$ ,  $O_2$  and He, ratio 4 : 1 : 10. In the case of transition metal oxides, the selectivity to propene was shown to correlate with the metal–oxygen bond strength. No such correlation was established in the case of rare earth metal oxides. It was concluded that the surface adsorbed oxygen reported to be associated with the rare earth oxides catalyst played the dominant role in the selectivity-determining step. Among the catalysts, chromium oxide was found to exhibit the best performance. At 350 °C, the propane conversion was 8.9% and selectivity to  $C_3H_6$  was 36.0%, while

at 450 °C the conversion was 13.7% and selectivity to  $C_3H_6$  was 48.1%. The selectivity to olefins was not high, perhaps due the presence of weakly bonded lattice or surface oxygen in the catalyst. Chromium oxide was reported to have weakly adsorbed oxygen species [12].

In this paper, the POD has been studied on metal pyrophosphates and phosphates catalysts. In a recent temperature-programmed desorption (TPD) study, these catalysts did not desorb oxygen up to 550 °C [13]. This suggested that they might not have oxygen species weakly adsorbed on the surface. In addition, metal pyrophosphates have lattice oxygen with a stronger bond than in metal oxides. Therefore, the former may show different selectivity patterns than the latter. Lattice oxygen of intermediate strength is required for high selectivity to olefins. Weakly bonded oxygen in the catalyst leads to overoxidation to  $CO_x$  while strongly bonded oxygen renders the catalysts inactive for the reaction. On the basis of the foregoing, the catalysts ( $M-P_2O_7$ , where M is V, Zr, Cr, Mg, Mn, Ni or Ce) were prepared and tested for the reaction. They are represented as  $M-P_2O_7$  although both pyrophosphate and phosphates may be present in the system [13]. Recently, a report from our laboratory has shown that metal pyrophosphates are active in the oxidative dehydrogenation of isobutane to isobutene [14].

## 2. Experimental

The catalysts ( $M-P_2O_7$ , where M is Ni, Ce, Mg, Zr, Cr, V or Mn) were prepared from their precursors:  $Ni(NO_3)_2 \cdot 6H_2O$  (Tech England),  $Ce(NH_4)_2(NO_3)_6$  (Fluka AG Buchs SG),  $Mg(NO_3)_2$  (Merck Germany),  $Zr(NO_3)_3$  (BDH, AnalaR),  $Cr(NO_3)_3 \cdot 9H_2O$  (Riedel De Haen 12232) and

\* To whom correspondence should be addressed.

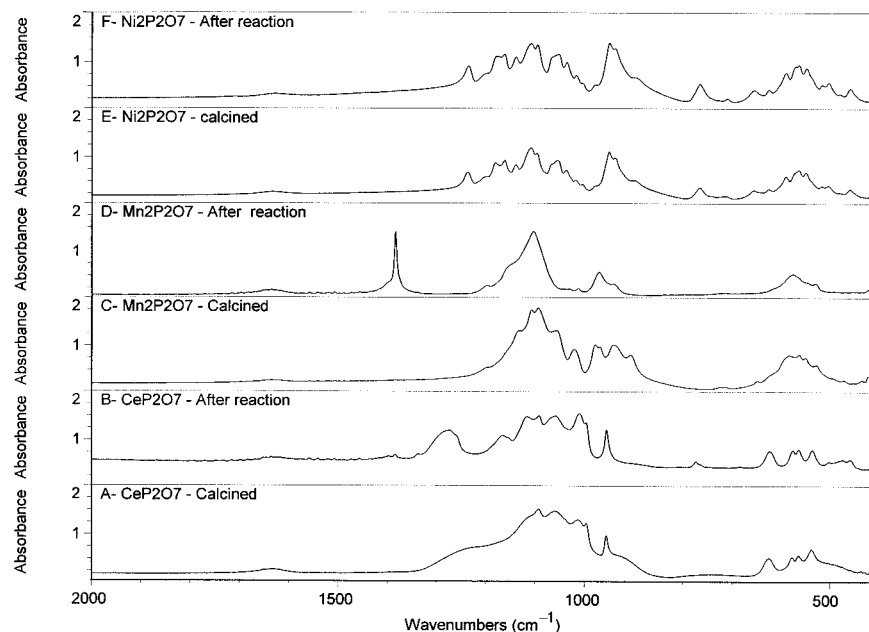


Figure 1. FTIR spectra of  $\text{Ce}_2\text{P}_2\text{O}_7$  (A, B),  $\text{Mn}_2\text{P}_2\text{O}_7$  (C, D) and  $\text{Ni}_2\text{P}_2\text{O}_7$  (E, F) catalysts.

$\text{NH}_4\text{VO}_3$  (BDH Germany), respectively. One mole of sodium pyrophosphate ( $\text{Na}_4\text{P}_2\text{O}_7$ ) was dissolved in 500 ml distilled water. One mole of each precursor was also dissolved in 500 ml. Both were at room temperature. Each of the resultant solution of the precursor (1 mol) was added dropwise to a continuously stirred solution of the pyrophosphate (1 mol) at  $70^\circ\text{C}$ . A precipitate of the corresponding metal pyrophosphate (or phosphate) was obtained. A complete precipitation test was carried out in each case by adding some drops of the precursor solution to the clear solution above the precipitate until no further precipitation was observed. The precipitate was kept in its solution until it completely settled down. It was then filtered, thoroughly washed and dried in an oven at  $100^\circ\text{C}$  for 72 h. Each of the dried catalysts was pressed into pellets, crushed and sieved into 20–40 mesh granules and calcined at  $600^\circ\text{C}$  for 3 h. The infrared spectra of both fresh and used catalysts were collected using Portage-460 Nicolet FTIR equipment. The pore volume, average pore diameter and surface areas of the catalysts were obtained using a Micromeritics ASAP-2000. X-ray diffraction patterns were determined on a Philips PW diffractometer with Cu  $\text{K}\alpha$  radiation. It was operated in the scanning mode with a step size of  $0.04^\circ$  and counting time of 1.0 s. The experimental setup and catalysts testing method are reported earlier [14].

### 3. Results and discussion

The catalysts surface areas, pore volumes and average pore diameters are shown in table 1. Another sample of the catalysts ( $\text{Ni}_2\text{P}_2\text{O}_7$ ,  $\text{Mn}_2\text{P}_2\text{O}_7$  and  $\text{CeP}_2\text{O}_7$ ) has been analyzed using FT-IR. Both fresh and spent catalysts were studied. Figure 1 shows two spectra for each catalyst. For each set, the spectrum at the bottom belongs to the fresh catalyst

Table 1  
Some physical properties of a sample of the catalysts.

Sample	Total (BET) surface area ( $\text{m}^2/\text{g}$ )	Pore volume ( $\text{cm}^3/\text{g}$ )	Average pore diameter ( $\text{\AA}$ )
$\text{CeP}_2\text{O}_7$	49.00	0.500	358.57
$\text{Mn}_2\text{P}_2\text{O}_7$	5.60	0.035	264.74
$\text{V}_4(\text{P}_2\text{O}_7)_3$	0.40	0.004	558.45
$\text{ZrP}_2\text{O}_7$	47.30	0.132	56.02
$\text{Ni}_2\text{P}_2\text{O}_7$	1.50	0.010	108.98
$\text{Mg}_2\text{P}_2\text{O}_7$	0.22	0.018	575.18

sample (before the reaction) while the spectrum at the top belongs to the same catalyst after the reaction. As a common observation for all used catalysts, adsorbed O–H peaks in the stretch vibrational mode are detected in the range of  $2500\text{--}3500\text{ cm}^{-1}$  [14]. The peaks that appeared in the range of  $900\text{--}1200\text{ cm}^{-1}$  are assigned to the  $\text{P}_2\text{O}_7$  group. In the FTIR spectra for  $\text{CeP}_2\text{O}_7$  (figure 1 (A) and (B)), a new peak was detected at a wave number of  $1280\text{ cm}^{-1}$  after the reaction. This peak could be attributed to a single bond stretching –C–. The  $\text{P}_2\text{O}_7$  group pattern becomes more intensive after the reaction. In the FTIR spectra for  $\text{Mn}_2\text{P}_2\text{O}_7$  (figure 1 (C) and (D)), another new peak was detected at a wave number of  $1380\text{ cm}^{-1}$ . This peak was correlated to deformation of a H–C–H group. Contrary to the case of  $\text{CeP}_2\text{O}_7$ ,  $\text{P}_2\text{O}_7$  in spectrum (D) is clearly separated. The FTIR spectra for  $\text{Ni}_2\text{P}_2\text{O}_7$  (figure 1 (E) and (F)) show practically the same pattern before and after the reaction. These spectra indicate that the participation of the  $\text{P}_2\text{O}_7$  group and the adsorption of hydrocarbon species in the reaction are different on the tested catalysts. The metal properties seem to play an important role in determining the characteristics of the catalysts.

The degrees of conversion and product distributions of each catalyst have been studied. As mentioned earlier, the reaction was conducted at 1 atm,  $450\text{--}550^\circ\text{C}$  and

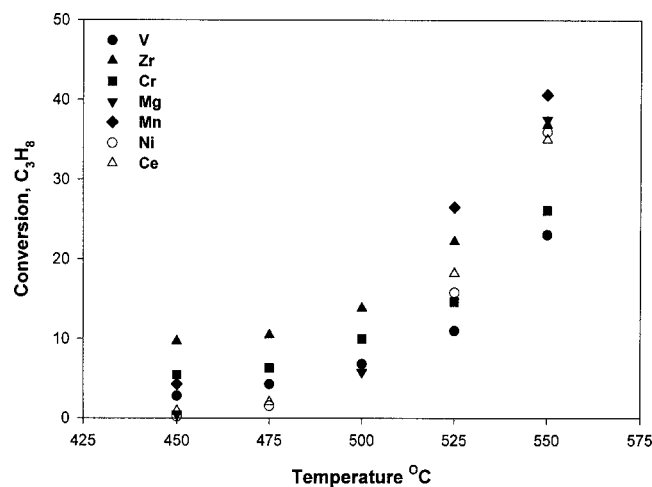


Figure 2. Propane degrees of conversion as functions of temperature from 450 to 550 °C.

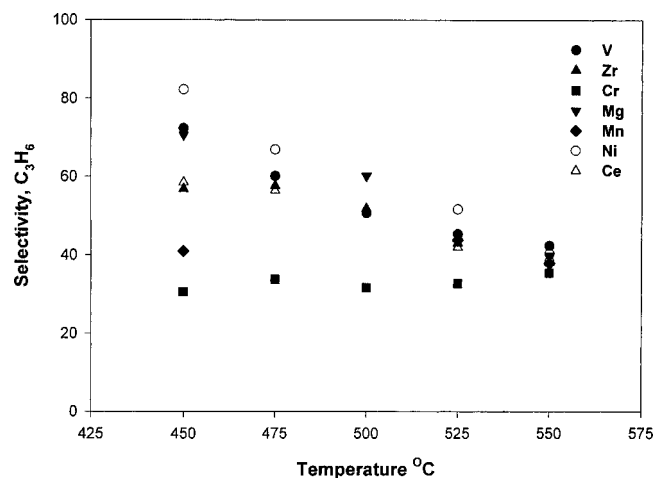


Figure 3. Selectivities to propene as functions of temperature from 450 to 550 °C.

Table 2  
Oxidative dehydrogenation of propane over  $\text{Mn}_2\text{P}_2\text{O}_7$ .

	Reaction temperature (°C)		
	450	525	550
<b>Conversion (%)</b>			
$\text{C}_3\text{H}_8$	4.3	26.5	40.7
$\text{O}_2$	37.8	77.9	88.6
<b>Selectivity (%)</b>			
$\text{C}_3\text{H}_6$	41.0	43.9	37.9
$\text{C}_2\text{H}_4$	15.2	30.9	34.2
$\text{CH}_4$	2.6	12.3	14.8
$\text{CO}_2$	13.2	1.8	1.1
$\text{CO}$	28.1	6.7	6.3
<b>Yield (%)</b>			
$\text{C}_3\text{H}_6$	1.8	11.6	15.4
$\text{C}_2\text{H}_4$	0.6	8.2	13.9
$\text{CO}_2$	0.6	0.5	0.4
$\text{CO}$	1.2	1.8	2.6
Carbon balance	102.5	100.5	96.5

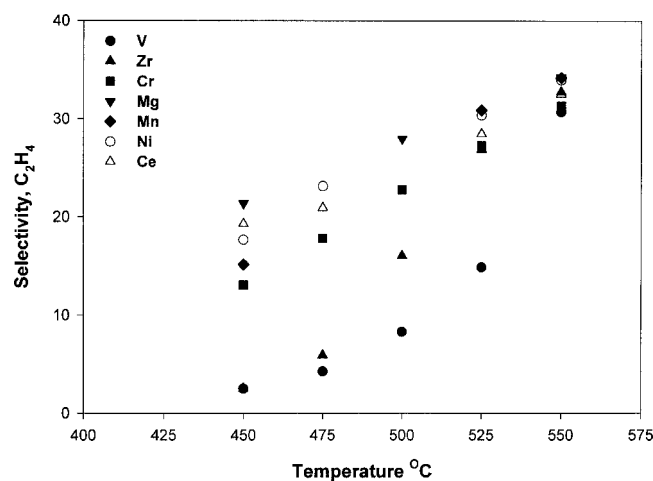


Figure 4. Selectivities to ethene as functions of temperature from 450 to 550 °C.

75  $\text{cm}^3/\text{min}$  feed flowrate (20  $\text{cm}^3/\text{min}$  propane, 5  $\text{cm}^3/\text{min}$  oxygen and the balance helium). Figure 2 shows the propane degree of conversion with temperature. At 450 °C the degree of conversion was between 0.2% for  $\text{Ni}_2\text{P}_2\text{O}_7$  and 9.7% for  $\text{ZrP}_2\text{O}_7$ . This indicates lower activities for the metal pyrophosphate than for supported metal oxides studied previously, where for instance, the degree of conversion of  $\text{Zr}_2\text{O}_3/\text{Al}_2\text{O}_3$  was 10.8% at 450 °C [10]. As shown in figure 2, the propane conversion increases with increase in temperature. At 550 °C,  $\text{V}_4(\text{P}_2\text{O}_7)_3$  showed lowest conversion of 23% while  $\text{Mn}_2\text{P}_2\text{O}_7$  has the highest value of 40.6%. Table 2 shows the product distributions of  $\text{Mn}_2\text{P}_2\text{O}_7$  at 450, 525 and 550 °C. The selectivities to propene for all the catalysts are shown in figure 3. The catalysts showed different behaviors. Those containing V, Zr, Mg, Mn, Ni and Ce showed decrease in selectivity to propene with increase in conversion of propane, a typical behavior associated with oxidative dehydrogenation reactions.  $\text{Cr}_4(\text{P}_2\text{O}_7)_3$  exhibited an unexpected little change in the selectivity to propene in

the temperature range. The Cr is expected to behave in a similar manner to V and Mn. Surprisingly, it produced mainly  $\text{C}_2\text{H}_4$  and  $\text{CO}_x$ .

Figure 4 shows that the selectivities to  $\text{C}_2\text{H}_4$  increase with increase in temperature. It is interesting to observe that the reaction produced mainly  $\text{C}_2\text{H}_4$  and  $\text{CH}_4$  as the selectivities to  $\text{CO}_x$  show general decrease with increase in temperature. As stated previously, the Cr catalyst produced mainly  $\text{C}_2\text{H}_4$  and  $\text{CO}_x$ . This is probably a result of surface adsorbed oxygen, which is reported to increase the selectivity to  $\text{C}_2\text{H}_4$  and  $\text{CO}_x$  due to an attack on either the propyl species or propene [15]. Figure 5 shows the total propene yield. The catalysts (indicated by their respective metals) may be ranked, based on olefins yield at 550 °C as  $\text{V}$  (16.9%) <  $\text{Cr}$  (17.5%) <  $\text{Ce}$  (25.1%) <  $\text{Zr}$  (26.2%) <  $\text{Ni}$  (26.8%) <  $\text{Mg}$  (27.9%) <  $\text{Mn}$  (29.3%). Figure 6 shows the selectivities to  $\text{CO}_x$ . The selectivities to  $\text{CO}_x$  generally decrease with increase in temperature, which is perhaps due to depletion of oxygen in the reaction at higher temperatures.

The reactivity of the lattice oxygen in the metal pyrophosphates could be estimated from the standard energy of for-

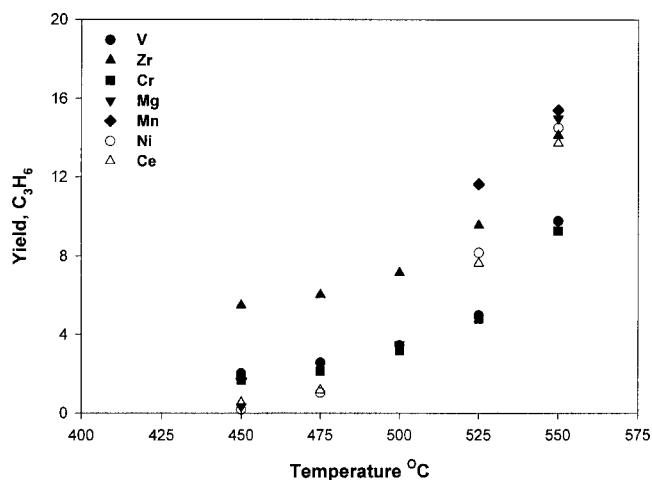
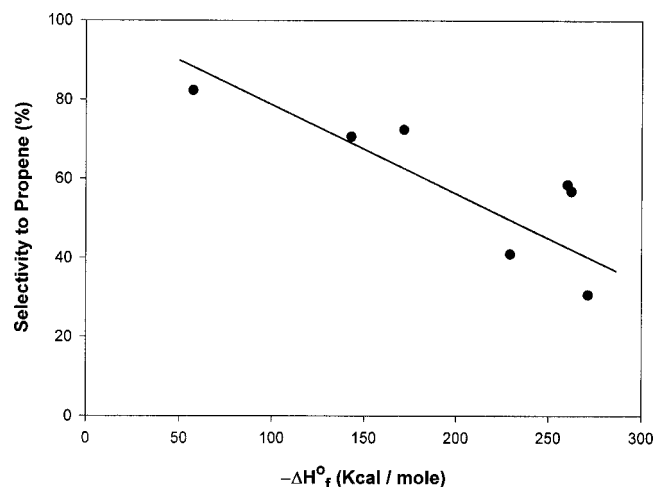
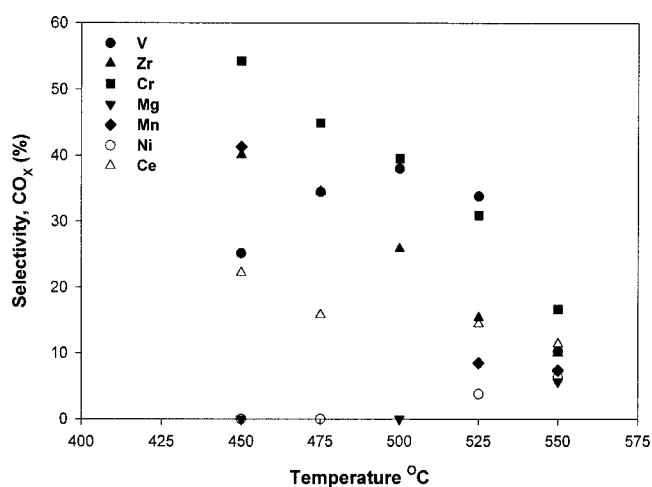


Figure 5. Propene yields as functions of temperature from 450 to 550 °C.

Figure 7. Selectivity to propene as function of  $\Delta H_f^0$  of the corresponding metal oxides.Figure 6. Selectivities to  $\text{CO}_x$  as functions of temperature from 450 to 550 °C.

mation of the corresponding metal oxides ( $\Delta H_f^0$ ). The higher the value of  $\Delta H_f^0$ , the stronger the bond of lattice oxygen and the less reducible the catalyst. Therefore, the higher the  $\Delta H_f^0$ , the more electrophilic the oxygen, which makes it more susceptible to attack electron-rich propyl species or propene molecule. The nature of the reaction of the propyl species determines the selectivity of the reaction. Consequently, this suggests decrease in selectivity to propene with increase in  $\Delta H_f^0$ , as shown in figure 7. In addition, the selectivity to propene may be reduced if the propene was not desorbed fast, as would be the case in more electrophilic environment. Although there is no outright correlation between the selectivity to propene and  $\Delta H_f^0$ , the figure suggests the important roles played by the lattice oxygen in the product distribution of the catalyst. Furthermore, this corroborates the earlier suggestion that the metal properties are important in determining the characteristics of the catalyst.

#### 4. Conclusion

Propane oxidative dehydrogenation has been studied on metal pyrophosphates. The metals used were V, Zr, Cr, Mg, Mn, Ni and Ce. The catalysts were active at 450–550 °C;  $\text{Mn}_2\text{P}_2\text{O}_7$  exhibited the highest activity (40.6% propane conversion), propene yield 15.4% and ethene yield of 13.9%. This system showed some promise as a catalyst in oxidative dehydrogenation of propane. However, it is not as active as the supported metal oxides we have studied earlier, due to the stronger metal–oxygen bond. The lattice oxygen appeared to play an important role in the selectivity-determining step of the reaction.

#### References

- [1] A. Corma, J.M. Lopez Neito and N.J. Paredes, *J. Catal.* 144 (1993) 425.
- [2] H.H. Kung and M.C. Kung, *Appl. Catal. A* 157 (1997) 105.
- [3] F. Cavani, G. Centi, F. Trifirò and R.K. Grasselli, *Catal. Today* 3 (1988) 185.
- [4] Y.C. Kim, W. Ueda and Y. Moro-oka, *Catal. Today* 13 (1992) 673.
- [5] D.L. Stern and R.K. Grasselli, *J. Catal.* 167 (1997) 550.
- [6] C. Mazzocchi, C. Aboumrar, C. Diagne, E. Tempesti, J.M. Herrmann and G. Thomas, *Catal. Lett.* 10 (1991) 181.
- [7] M. Ai, *Catal. Today* 12 (1992) 679.
- [8] Y. Takita, H. Yamashita and K. Moritaka, *Chem. Lett.* (1989) 1903.
- [9] Z.M. Fang, Q. Hong, Z.H. Zhou, S.J. Dai, W.Z. Weng and H.L. Wan, *Catal. Lett.* 61 (1999) 39.
- [10] S.M. Al-Zahrani, B.Y. Jibril and A.E. Abasaheed, *Ind. Eng. Chem. Res.* 39 (2000) 4070.
- [11] S.M. Al-Zahrani, B.Y. Jibril and A.E. Abasaheed, *Ind. Eng. Chem. Res.* submitted.
- [12] M. Iwamoto, Y. Yoda, N. Yamazoe and T. Seiyama, *J. Phys. Chem.* 82 (1978) 2564.
- [13] Y. Takita, K. Sano, K. Kurosaki, N. Kawata, H. Nishiguchi, M. Ito and T. Ishihara, *Appl. Catal. A* 169 (1998) 49.
- [14] S.M. Al-Zahrani, N.O. Elbashir, A.E. Abasaheed and M. Abdulwahid, *Catal. Lett.* 69 (2000) 65.
- [15] M. Bearn and O. Buyevskaya, *Catal. Today* 45 (1998) 13.